

# UC Davis

## UC Davis Previously Published Works

### Title

Davis-Beirut Reaction: A Photochemical Brønsted Acid Catalyzed Route to N-Aryl 2H-Indazoles

### Permalink

<https://escholarship.org/uc/item/9722b14f>

### Journal

Organic Letters, 21(15)

### ISSN

1523-7060

### Authors

Kraemer, Niklas  
Li, Clarabella J  
Zhu, Jie S  
[et al.](#)

### Publication Date

2019-08-02

### DOI

10.1021/acs.orglett.9b02213

Peer reviewed



Published in final edited form as:

Org Lett. 2019 August 02; 21(15): 6058–6062. doi:10.1021/acs.orglett.9b02213.

## Davis–Beirut Reaction: A Photochemical Brønsted Acid Catalyzed Route to *N*-Aryl 2*H*-Indazoles

Niklas Kraemer<sup>†,§</sup>, Clarabella J. Li<sup>†,§</sup>, Jie S. Zhu<sup>†</sup>, Julio M. Larach<sup>†</sup>, Ka Yi Tsui<sup>†</sup>, Dean J. Tantillo<sup>†</sup>, Makhlu J. Haddadin<sup>‡</sup>, Mark J. Kurth<sup>\*,†</sup>

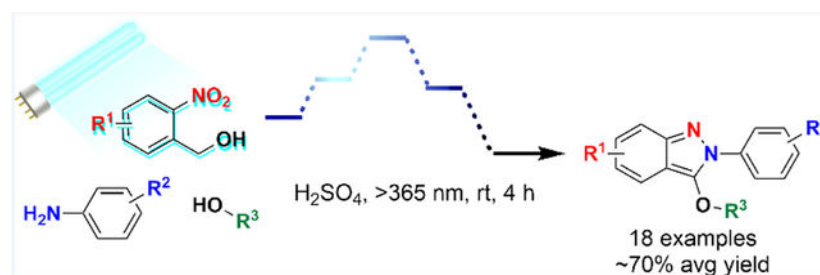
<sup>†</sup>Department of Chemistry, University of California Davis, 1 Shields Avenue, Davis, California 95616, United States

<sup>‡</sup>Department of Chemistry, American University of Beirut, Beirut, Lebanon

### Abstract

The Davis–Beirut reaction provides access to 2*H*-indazoles from aromatic nitro compounds. However, *N*-aryl targets have been traditionally challenging to access due to competitive alternate reaction pathways. Previously, the key nitroso imine intermediate was generated under alkaline conditions, but as reported here, the photochemistry of *o*-nitrobenzyl alcohols empowered Brønsted acid catalyzed conditions for accessing *N*-aryl targets. Anilines and alkyl amines give different outcomes under optimized conditions; the proposed mechanism was studied using quantum chemical calculations.

### Graphical Abstract



Nitrogen-containing heterocycles are medicinal chemistry and natural product staples, and the indazole core forms the backbone of a variety of biologically important molecules, having shown analgesic,<sup>1</sup> antiviral,<sup>2</sup> antichastic,<sup>3</sup> antitumor,<sup>4</sup> and anticancer properties.<sup>5</sup> Indeed, indazole derivatives are privileged among nitrogen heterocycles and they afford access to the corresponding indazolones,<sup>6</sup> another family of biologically relevant compounds.<sup>6a,b</sup> Typically, indazoles and indazolones are synthesized with the N–N bond

\*Corresponding Author: mjkurth@ucdavis.edu.

§N.K. and C.J.L. contributed equally.

Supporting Information

The Supporting Information is available free of charge on the ACS Publications website at DOI: 10.1021/acs.orglett.9b02213. Experimental procedures, compound characterization, <sup>1</sup>H and <sup>13</sup>C NMR spectra, computational details (PDF)

Notes

The authors declare no competing financial interest.

already in place, sometimes with the aid of transition metal catalysts,<sup>7</sup> using the Cadogan cyclization,<sup>8</sup> or via redox manipulation strategies.<sup>9</sup>

The Davis–Beirut reaction (DBR) is a redox neutral method for the conversion of *o*-nitrobenzyl amines to 2H-indazoles.<sup>10</sup> The formation of an N–N bond is a key step in the DBR, but this reaction poorly accommodates reactions with anilines to form the corresponding N-aryl products (Scheme 1A),<sup>11</sup> even though the N–N bond forming reaction between anilines and aryl nitroso groups is well established in the Mills reaction.<sup>12</sup> In many cases, C–N bond cleavage is favored over N–N bond formation when anilines are used in the DBR.<sup>11b,13</sup> This issue likely arises from the fact that the Mills reaction is acid catalyzed while the DBR is typically carried out under alkaline conditions. This limitation has been disappointing because it significantly impacts the substrate scope of the DBR. We speculated that the presence of a Brønsted acid would significantly impact the reactivity of nitroso intermediates 2 and 3 (Scheme 2), enabling Mills-like N–N bond formation. The traditional DBR is, unfortunately, incompatible with Brønsted acids because KOH is used to generate the nitroso species. However, our group recently demonstrated that the key nitroso imine intermediate can be generated in situ under photochemical conditions<sup>14</sup> in aqueous PBS solution and subsequently intercepted by primary amines (Scheme 2).<sup>15</sup> Kambe<sup>16</sup> and Chen<sup>17</sup> more recently reported similar photo-chemical methods leading to indazolones, but it should be noted that accessing N-aryl products using their methods remains problematic. Development of these photochemical methods gave us the experimental flexibility required to study the highly reactive nitroso intermediates under Brønsted acid catalysis (Scheme 1B).

When we treated 1 equiv of *o*-nitrobenzyl alcohol, 1 equiv of aniline, catalytic amounts of H<sub>2</sub>SO<sub>4</sub>, and <sup>i</sup>PrOH in a quartz test tube with >365 nm light<sup>18</sup> for 24 h, indazole 5 was obtained in 61% yield. We were delighted by this result because secondary alcohols have never been successfully incorporated using this chemistry due to their reduced nucleophilicity relative to MeOH or EtOH.<sup>19</sup> Indeed, exploiting the nonreactivity of <sup>i</sup>PrOH with nitroso imines was central in the strategy we previously employed for direct indazolone synthesis via the DBR.<sup>11b</sup> Incorporating N-aryl and O-isopropyl substituents into this heterocyclic framework represents the most challenging substitution pattern for the DBR.

After optimizing the reaction (see Supporting Information [SI]; Table S1 for details), the substrate scope was explored (Figure 1). EtOH, MeOH, cyclopentanol, and 2-methoxyethanol provided indazoles (6–9) in excellent yields, but allyl/propargyl alcohol and *m*-cresol failed to give indazoles 10a/10b and 11, respectively. When carried out in tert-butanol, indazole 12 was not obtained. Instead, N-aryl indazolone 12a (64%; 12b in 71% from *p*-anisidine) was formed, either by addition of H<sub>2</sub>O instead of tert-butanol to 57 (see Figure 4) or by acid-mediated hydrolysis of indazole 12 (see SI for additional discussion). Obtaining 12a and 12b represents a major improvement over other direct methods for N-aryl indazolone synthesis (see Scheme 1A).<sup>11b,15–17</sup> While *p*-aminopyridine did not give 13, naphthalen-2-amine successfully gave 14 in 75% yield. Comparing 15 vs 16 highlights the role of reactive intermediate steric demands, while comparing 18 vs 19a/19b/20 highlights substrate electronic effects on reaction outcome. Due to the short reaction time and limited UV exposure, starting material aryl halides did not undergo bond scission during the course

of the reaction;<sup>15,17</sup> the successful preparation of indazoles 21–26 demonstrates the tolerance of various halogens. While *p*-iodoaniline and *m*-chloroaniline give the corresponding indazoles in good yield (77% and 75%, respectively), the use of *o*- and *m*-bromoaniline resulted in lower yields (36% and 43%, respectively). Finally, when the synthesis of 5 was performed on a 300 mg scale, an 82% yield was obtained.

Intramolecular DBRs are expected to give polycyclic indazoles when anilines with tethered alcohols are used due to intramolecular incorporation of the alcohol nucleophile (Figure 2).<sup>20</sup> However, since alkoxy indazoles are also known to undergo hydrolysis to indazolones when treated with a Brønsted acid, it was not straightforward to predict the outcome under acid-mediated reaction conditions.<sup>21</sup> Indeed, when 27 was reacted with 1 in *i*PrOH, indazole 28 and indazolone 29 were obtained in 23% and 25% yields, respectively. With the realization that the synthesis of 29 traditionally required a three-step sequence (N-alkylation, DBR, then KI/ ),<sup>6c</sup> we attempted to improve the yield of the indazolone product by screening additional solvents: DCM, THF, and DMF. While both DCM and THF gave complex mixtures, DMF gave indazolone 29 in 73% yield; subsequent reactions were performed in parallel using both *i*PrOH and DMF. Using 30 in the reaction gave 6–5–7–6 fused indazole 31 in 87% and 61% yields in *i*PrOH and DMF, respectively; indazolone 32 was not formed in either solvent. When secondary alcohol 33 was employed as a substrate, the reaction gave 37% of indazole product 34 and 0% of the indazolone product 35 (*i*PrOH as solvent). When DMF was used as the solvent, 13% of 34 and 0% of 35 were obtained. While using *tert*-butyl alcohol in the intermolecular reaction exclusively gave indazolone 12a/12b, using tertiary alcohol-containing substrate 36 surprisingly only gave fused indazole product 37 in 64% with *i*PrOH and 86% with DMF. Even though *m*-cresol did not participate in the intermolecular example to give 11, the reaction of 2-aminophenol (39) as a substrate with 1 in *i*PrOH gave the desired 6–5–5–6 fused indazole 40, albeit in only 15% yield due to the formation of 41 (39%) as a side product. When the reaction was carried out in DMF, the yield of 40 slightly increased to 28%. The surprising lack of formation of 38 led us to wonder whether indazolone 29 arose via an acid-mediated process from polycyclic indazole 28 or from direct cyclization at the hemiaminal stage (Figure 4; Pathway A).

Furthermore, as the problems with electron-rich anilines foreshadowed, employing butylamine instead of aniline failed to provide the corresponding indazole product (Scheme 3). When 0.5 equiv of butylamine was used, a complex mixture was obtained. In contrast, using 1 equiv of butylamine gave 2H-indazole N-oxide 42 in 21% yield<sup>13</sup> and using 2 equiv of butylamine gave indazolone 43 in 63% yield.<sup>15</sup>

To set the stage for constructing a mechanistic model for this reaction, a better understanding of the interactions of 3 and Brønsted acid was needed. Since nitroso imine 3 has the potential to be protonated at the nitroso oxygen, nitroso nitrogen, or imine nitrogen, we used quantum chemical calculations to study all three cases (Figure 3). Structures were optimized with the PCM(DMSO)-M06–2X/6–31+G(d,p)<sup>22</sup> and PCM(DMSO)-B3LYP-D3(BJ)/6–31+G(d,p)<sup>23</sup> density functional theory (DFT) methods. The geometries of the lowest energy conformers for each structure were optimized with DFT after systematic conformational searches were performed using Spartan10 (see SI for details). At equilibrium, protonation of the imine nitrogen is clearly favored over protonation of the

nitroso group at either N or O: 45 was thermodynamically favored over 44 by 31.6 kcal/mol and over 46 by 12.3 kcal/mol.

There are three known productive pathways leading to different heterocycles from the same nitroso intermediates (Figure 4): Pathway A leads to indazolones,<sup>11b</sup> Pathway B leads to 2H-indazole N-oxides,<sup>13</sup> and Pathway C leads to 3-alkoxy 2H-indazoles.<sup>10,11</sup> We studied all three pathways to understand the divergent reactivity between alkyl and aryl amines. First, Pathway B reaction energetics for both N-alkyl and N-aryl analogues were examined and ring closure to give the corresponding 2H-indazole N-oxide was found to be kinetically feasible at room temperature for both substrates, although the N-aryl case has a higher barrier (Figure 4; Pathway B).<sup>13</sup> The 2H-indazole N-oxide product from this cyclization is thermodynamically downhill in both cases, but less so for the aryl case. Consequently, ring opening back to the nitroso imine is more likely with N-aryl substrates.

Next, we examined ring closure reactions for hemiaminals and hemiaminal ethers (Figure 4, Pathways A and C). For the N-alkyl analogues, all modes of cyclization are predicted to be kinetically feasible at room temperature, but Pathways A and C have higher predicted barriers than Pathway B. In addition, charge separated N–N cyclization intermediates 53 and 66 are predicted to be formed in uphill processes. After the ring closing events for Pathways A and C, we expect that solvent-assisted proton transfer leads to the neutral cyclization products (54 and 67, which are thermodynamically downhill).

For N-aryl analogues, we failed to identify any productive transition state structures for Pathways A and C. We also were unable to locate 49 or 62 as minima on the potential energy surface; i.e. their N–N bonds are prone to barrierless cleavage. To estimate the difficulty of such an N–N cyclization, we optimized the geometries of 49 and 62 while constraining the N–N distance (1.558 Å). Their relative energies exceed 20 kcal/mol, suggesting that their formation is neither kinetically nor thermodynamically favorable. We also considered the possibility of a concerted but asynchronous reaction that combines the cyclization and internal proton transfer events, thereby avoiding the formation of the charge separated cyclized species, but predicted barriers exceeded 27 kcal/mol for both Pathways A and C for the N-aryl analogues (see SI for details). In all cases examined, cyclizations for N-alkyl analogues had lower barriers and were more exergonic.

Based on our calculations, it is reasonable to expect that N–N bond formation from hemiaminal intermediates is not responsible for the N-aryl indazolones presented in Figures 1 and 2. Instead, they must be derived from Brønsted acid catalyzed indazole rearrangements. Indeed, the computational results lead us to suggest that N–N bond formation generally proceeds via Pathway B for N-aryl substrates. The proposed mechanistic model for the work described here is represented by  $1 \rightarrow 2 \rightarrow 48 \rightarrow 55 \rightarrow 57 \rightarrow \text{indazole}$ , where  $2 \rightarrow 48 \rightarrow 55$  and  $57 \rightarrow \text{indazole}$  are catalyzed by the Brønsted acid. This mechanistic model is fully consistent with the poor performance of alkyl amines because their nucleophilicity enables competing Pathway A. We tested this proposed mechanistic model by subjecting N-oxide 42 to the optimized reaction conditions in MeOH, which provided the expected 3-methoxy-2H-indazole product in 50% yield, whereas previously heat was required for this transformation.<sup>13</sup> Although using an aryl N-oxide

would have been preferred, they could not be isolated without significant decomposition due to their ring opening back to nitroso imine.<sup>13</sup>

Our results clarify the role of the Brønsted acid in this transformation. Since the predicted equilibrium suggests that the formation of 2*H*-indazole *N*-oxide is not being catalyzed and catalyzing <sup>1</sup>PrOH addition to nitroso imine is also not predicted to be productive for accessing the 3-isopropoxy 2*H*-indazoles, the most reasonable role of Brønsted acid in this reaction is as follows. First, it catalyzes aniline's condensation with nitroso benzaldehyde 2 to give nitroso imine 55. Second, when alcohol reacts with 55 to give unproductive hemiaminal ether 61, the Brønsted acid accelerates C–O bond cleavage/C=N bond formation to regenerate nitroso imine 55, which gives 55 additional opportunities to cyclize to *N*-oxide 57. Brønsted acid also catalyzes the reaction of alcohol solvent with *N*-oxide 57 to deliver 3-alkoxy 2*H*-indazole by protonating at the oxygen of 57. Thus, in contrast to our initial hypothesis vis-à-vis the Mills reaction, N–N bond formation is not Brønsted acid catalyzed in this reaction. Indeed, the originally discovered Davis–Beirut reaction involves base-mediated conversion of 58 to 3-alkoxy 2*H*-indazole; i.e., N–N bond formation does not require a Brønsted acid.

In summary, the photochemistry of 1 unlocks previously incompatible reaction conditions for the DBR; the consequence is greatly improved DBR flexibility and synthetic utility. Inter- and intramolecular examples were both probed experimentally, and the mechanistic model of this Brønsted acid catalyzed reaction was studied using quantum chemical calculations. A Brønsted acid facilitates the reaction, but it does not directly catalyze N–N bond formation. Rather, it catalyzes formation of 2 to 55 and conversion of 57 to alkoxy 2*H*-indazole.

## Supplementary Material

Refer to Web version on PubMed Central for supplementary material.

## ■ ACKNOWLEDGMENTS

The authors gratefully acknowledge financial support from the National Institutes of Health (DK072517 and DK067003 to M.J.K.) and NSF XSEDE program (CHE030089 to D.J.T.). Funding for NMR spectrometers was provided by National Science Foundation (DBI722538 and CHE9808183) and National Institute of Environmental Health (ES005707–13). N.K. is supported by the UC Davis Provost's Undergraduate Fellowship. J.S.Z. is supported by the UC Davis Tara K. Telford CF Fund, UC Davis Dissertation Year Fellowship, and R. Bryan Miller Graduate Fellowship. The authors thank the Shaw group (UC Davis) for use of their Teledyne ISCO CombiFlash and Mr. David Favela (Olson group, UC Davis) for assistance with synthesis of 36.

## ■ REFERENCES

- (1). Fletcher S; McIver E; Lewis S; Burkamp F; Leech C; Mason G; Boyce S; Morrison D; Richards G; Sutton K; Brian Jones A *Bioorg. Med. Chem. Lett* 2006, 16, 2872. [PubMed: 16563760]
- (2). Kim D; Wang L; Caldwell CG; Chen P; Finke PE; Oates B; MacCoss M; Mills SG; Malkowitz L; Gould SL; DeMartino JA; Springer MS; Hazuda D; Miller M; Kessler J; Danzeisen R; Carver G; Carella A; Holmes K; Lineberger J; Schleif WA; Emini EA *Bioorg. Med. Chem. Lett* 2001, 11, 3103. [PubMed: 11720852]
- (3). Vega MC; Rolon M; Montero-Torres A; Fonseca-Berzal C; Escario JA; Gomez-Barrio A; Galvez J; Marrero-Ponce Y; Aran VJ *Eur. J. Med. Chem* 2012, 58, 214. [PubMed: 23124218]

- (4). Wang H; Han H; Von Hoff DD *Cancer Res.* 2006, 66, 9722. [PubMed: 17018631]
- (5). Kawanishi N; Sugimoto T; Shibata J; Nakamura K; Masutani K; Ikuta M; Hirai H *Bioorg. Med. Chem. Lett* 2006, 16, 5122. [PubMed: 16876403]
- (6) (a). Haddadin MJ; Conrad WE; Kurth MJ *Mini-Rev. Med. Chem* 2012, 12, 1293. [PubMed: 23092440] (b)Schmidt A; Beutler A; Snovydovych B *Eur. J. Org. Chem* 2008, 2008, 4073. (c)Donald MB; Conrad WE; Oakdale JS; Butler JD; Haddadin MJ; Kurth MJ *Org. Lett* 2010, 12, 2524. [PubMed: 20438102] (d)Zhu C; Kalin AJ; Fang L *Acc. Chem. Res* 2019, 52, 1089. [PubMed: 30943015]
- (7) (a). Halland N; Nazare M; R'kyek O; Alonso J; Urmann M; Lindenschmidt A *Angew. Chem., Int. Ed* 2009, 48, 6879.(b)Jin T; Yamamoto Y *Angew. Chem., Int. Ed* 2007, 46, 3323.(c)Shamsabadi A; Chudasama V *Chem. Commun* 2018, 54, 11180.(d)Thome I; Besson C; Kleine T; Bolm C *Angew. Chem., Int. Ed* 2013, 52, 7509.
- (8) (a). Genung NE; Wei L; Aspnes GE *Org. Lett* 2014, 16, 3114. [PubMed: 24848311] (b)Nykaza TV; Harrison TS; Ghosh A; Putnik RA; Radosevich AT *J. Am. Chem. Soc* 2017, 139, 6839. [PubMed: 28489354] (c)Schoene J; Bel Abed H; Schmieder P; Christmann M; Nazare M *Chem. - Eur. J* 2018, 24, 9090. [PubMed: 29644761]
- (9) (a). Correa A; Tellitu I; Domínguez E; SanMartin R *J. Org. Chem* 2006, 71, 3501. [PubMed: 16626131] (b)Lin W; Hu M-H; Feng X; Cao C-P; Huang Z-B; Shi D-Q *Tetrahedron* 2013, 69, 6721.(c)Yu D-G; Suri M; Glorius FJ *Am. Chem. Soc* 2013, 135, 8802.
- (10). Kurth MJ; Olmstead MM; Haddadin MJ *J. Org. Chem* 2005, 70, 1060. [PubMed: 15675871]
- (11) (a). Mills AD; Nazer MZ; Haddadin MJ; Kurth MJ *J. Org. Chem* 2006, 71, 2687.(b)Zhu JS; Kraemer N; Shatskikh ME; Li CJ; Son J-H; Haddadin MJ; Tantillo DJ; Kurth MJ *Org. Lett* 2018, 20, 4736. [PubMed: 30067041]
- (12). Merino E *Chem. Soc. Rev* 2011, 40, 3835. [PubMed: 21409258]
- (13). Zhu JS; Li CJ; Tsui KY; Kraemer N; Son J-H; Haddadin MJ; Tantillo DJ; Kurth MJ *J. Am. Chem. Soc* 2019, 141, 6247. [PubMed: 30912441]
- (14) (a). Klan P; Solomek T; Bochet CG; Blanc A; Givens R; Rubina M; Popik V; Kostikov A; Wirz J *Chem. Rev* 2013, 113, 119. [PubMed: 23256727] (b)Il'ichev YV; Schworer MA; Wirz JJ *Am. Chem. Soc* 2004, 126, 4581.(c)Gaplovsky M; Il'ichev YV; Kamdzhilov Y; Kombarova SV; Mac M; Schworer MA; Wirz J *Photochemical & Photobiological Sciences* 2005, 4, 33. [PubMed: 15616689]
- (15). Zhu JS; Kraemer N; Li CJ; Haddadin MJ; Kurth MJ *J. Org. Chem* 2018, 83, 15493. [PubMed: 30468072]
- (16). Yang T; Lu H; Qiu R; Hong L; Yin S-F; Kambe N *Chem. - Asian J* 2019, 14, 1436. [PubMed: 30838763]
- (17). Nie H-J; Guo A-D; Lin H-X; Chen X-H *RSC Adv.* 2019, 9, 13249.
- (18). Aung T; Liberko CA *J. Chem. Educ* 2014, 91, 939.
- (19). Phan TB; Breugst M; Mayr H *Angew. Chem., Int. Ed* 2006, 45, 3869.
- (20). Butler JD; Solano DM; Robins LI; Haddadin MJ; Kurth MJ *J. Org. Chem* 2008, 73, 234. [PubMed: 18052193]
- (21). Conrad WE; Fukazawa R; Haddadin MJ; Kurth MJ *Org. Lett* 2011, 13, 3138. [PubMed: 21612219]
- (22). Zhao Y; Truhlar DG *Theor. Chem. Acc* 2008, 120, 215.
- (23) (a). Cammi R; Mennucci B; Tomasi J In *Computational Chemistry: Reviews of Current Trends*; Leszczynski J, Ed.; World Scientific Publishing Co. Pte. Ltd.: Singapore, 2003; Vol. 8.(b)Becke AD *J. Chem. Phys* 1993, 98, 5648.(c)Grimme S; Ehrlich S; Goerigk LJ *Comput. Chem* 2011, 32, 1456.(d)Lee C; Yang W; Parr RG *Phys. Rev. B: Condens. Matter Mater. Phys* 1988, 37, 785. (e)Miehlich B; Savin A; Stoll H; Preuss H *Chem. Phys. Lett* 1989, 157, 200.

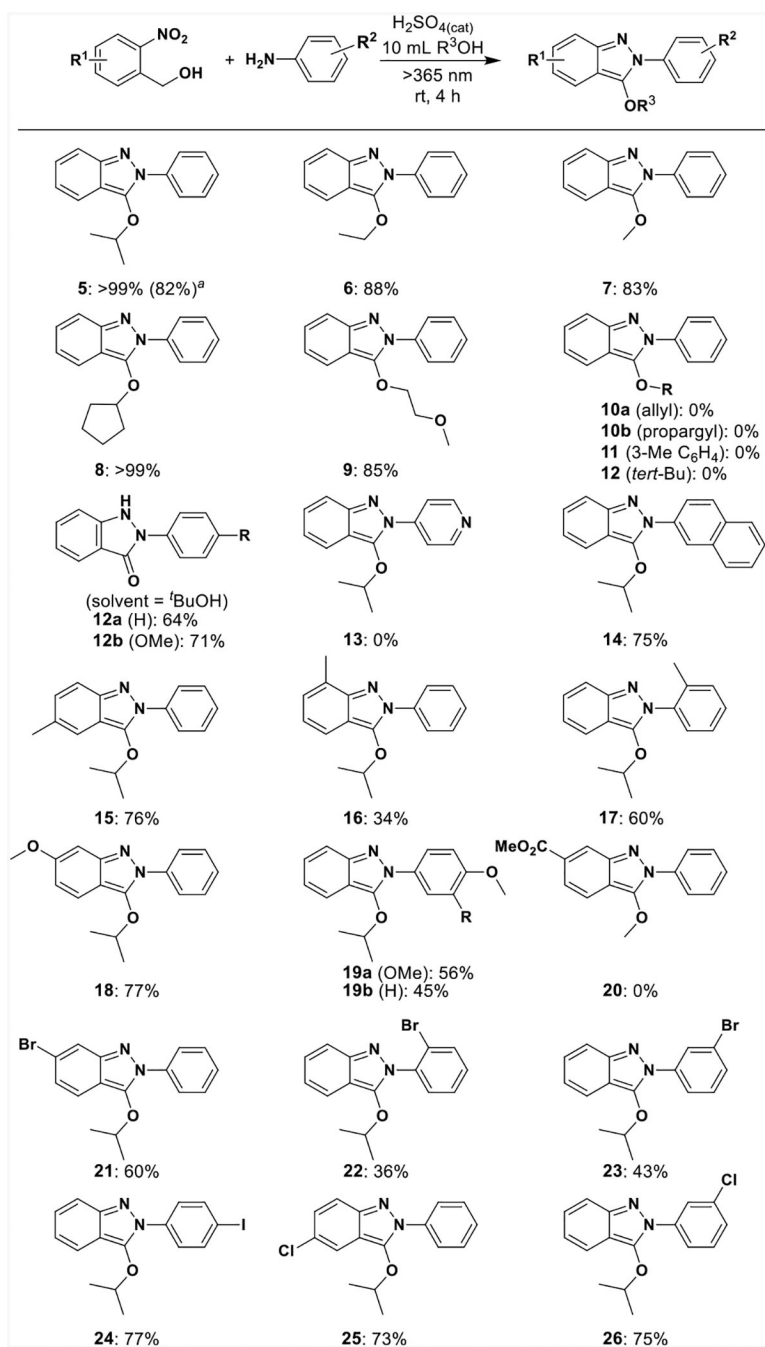


**Figure 1.** N-Aryl 2H-indazole synthesis. Reaction conditions: ThermalSpa photolysis of *o*-nitrobenzyl alcohol (0.5 mmol, 1 equiv), aniline (0.25 mmol, 0.5 equiv), alcohol solvent (10 mL), H<sub>2</sub>SO<sub>4</sub> (10  $\mu$ L), rt, 4 h. Isolated yields are reported. <sup>a</sup> 300 mg scale reaction.



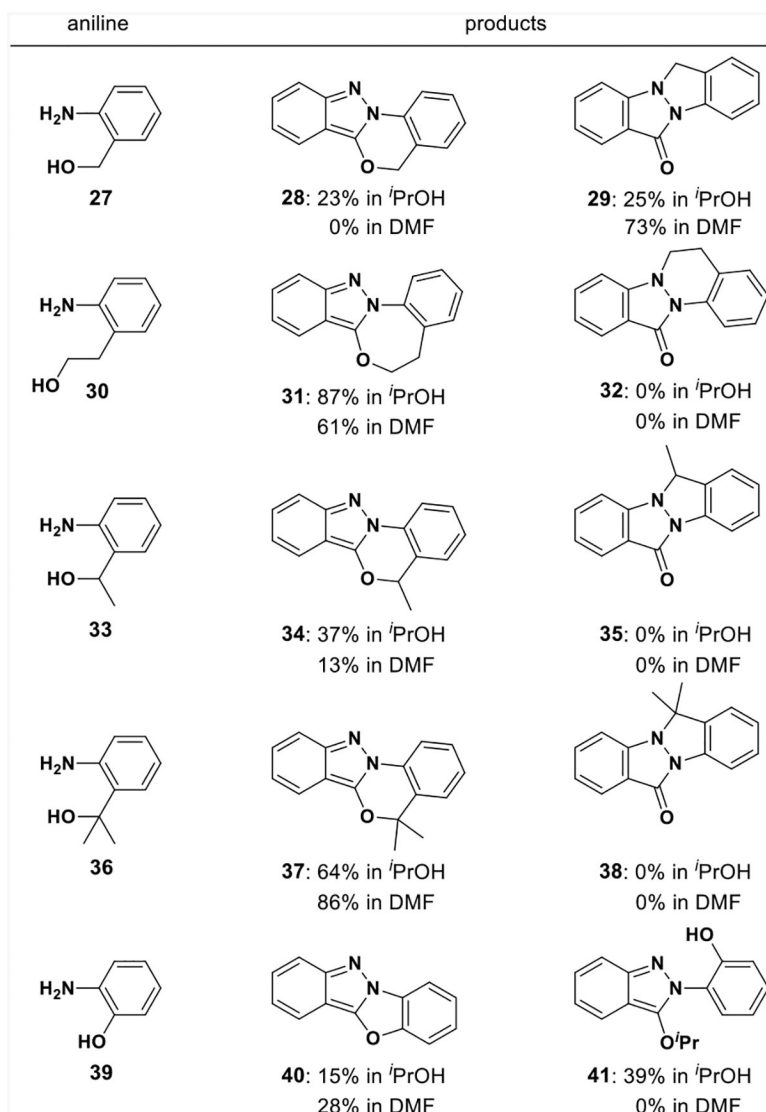


**Figure 2.** Tethered alcohol reactivity. Reaction conditions: Thermal-Spa photolysis of 1 (0.5 mmol, 1 equiv), amine (0.25 mmol, 0.5 equiv), DMF or *i*PrOH (10 mL), H<sub>2</sub>SO<sub>4</sub> (10 μL), rt, 4 h. Isolated yields are reported.

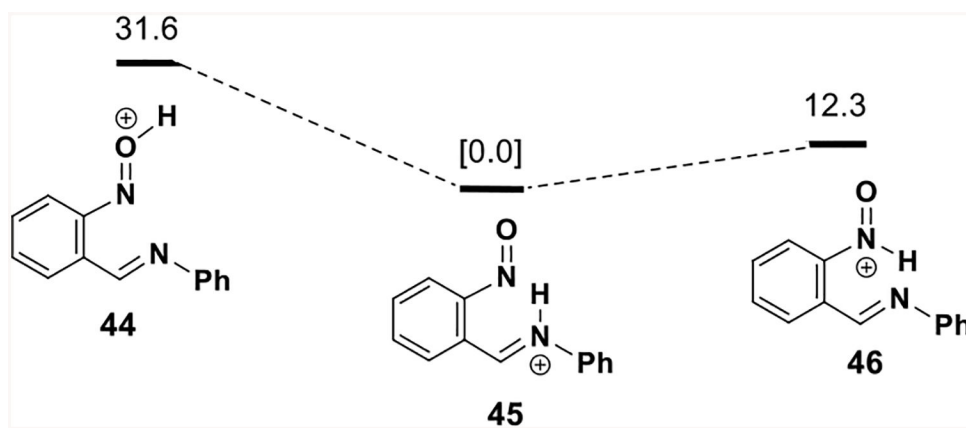


**Figure 3.**  
Different modes of nitroso imine protonation.

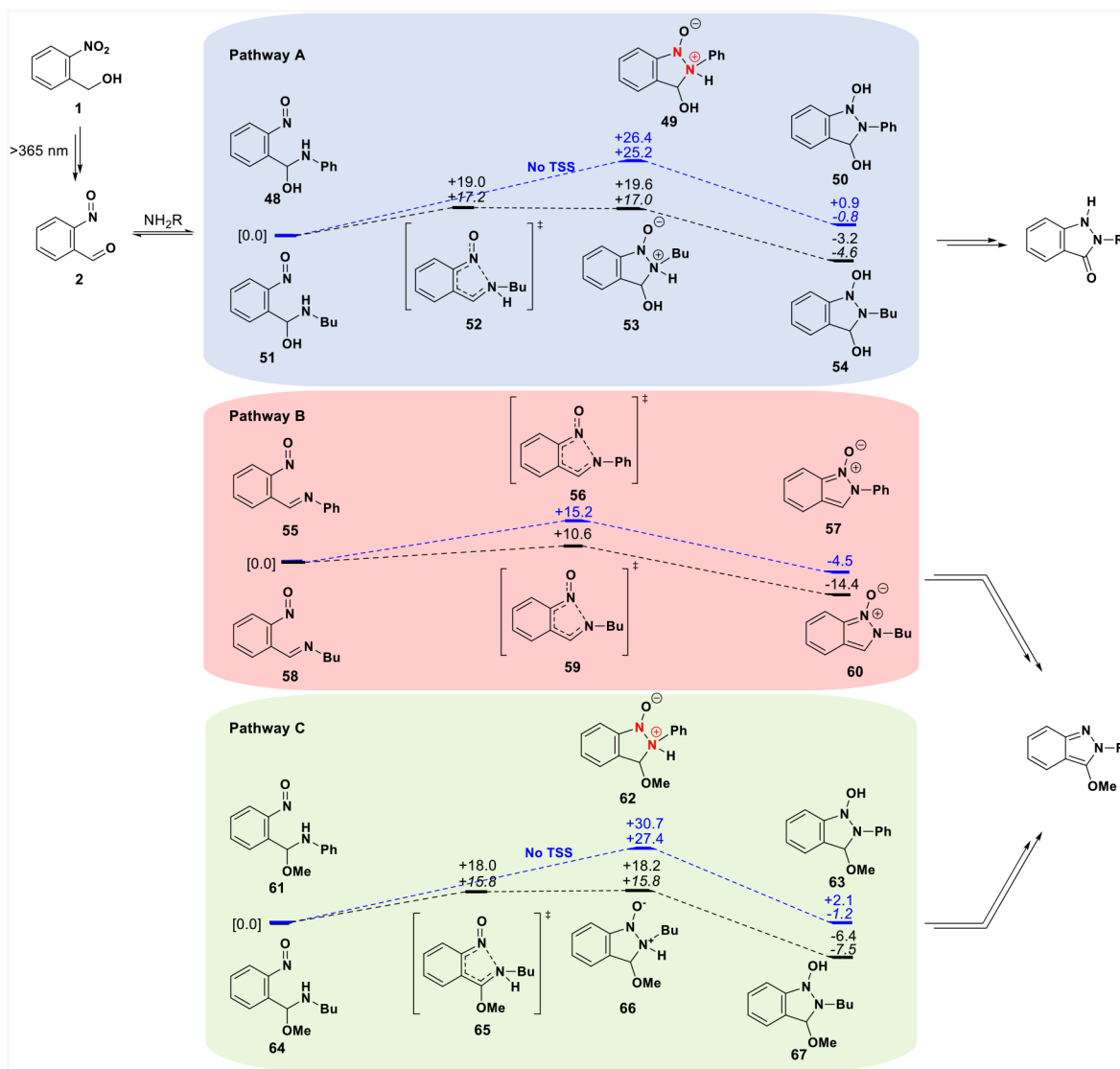
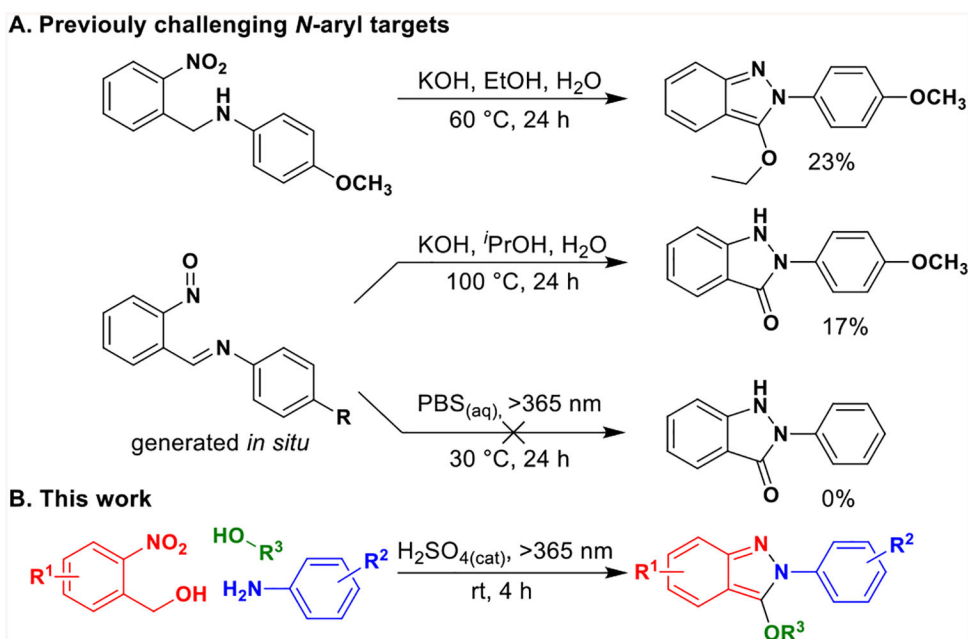
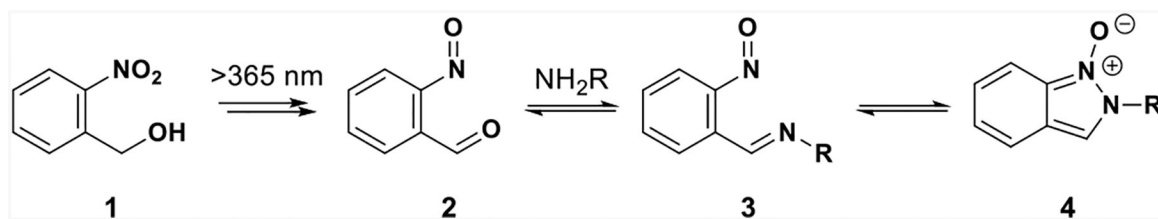


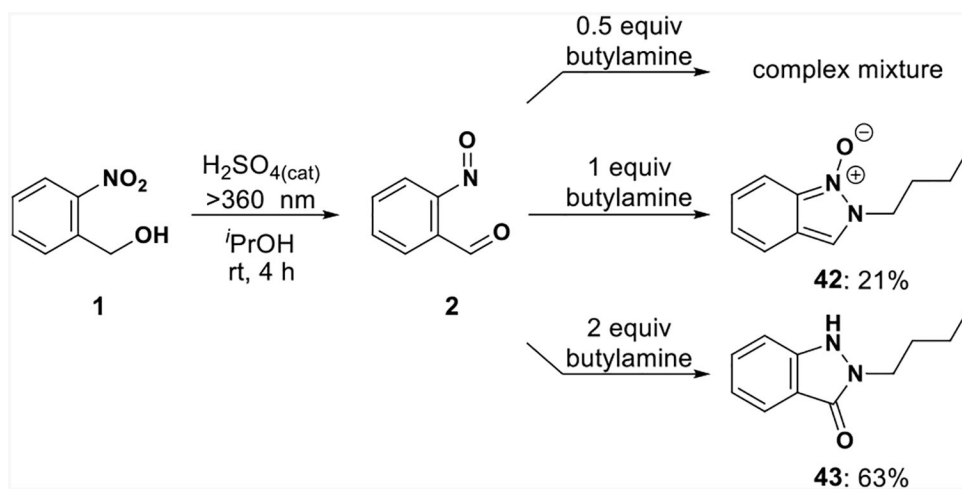
**Figure 4.** Different modes of cyclization. Reported here are free energies in units of kcal/mol, calculated at PCM(DMSO)-M06-2X/6-31+G(d,p). Electronic energies are shown in italic. Energies in blue and black are for phenyl and butyl reactions, respectively. Constrains are applied to the nitrogen atoms (in red) during geometry optimization.



**Scheme 1.**  
N-Aryl Targets via the DBR



**Scheme 2.**  
Generating Key Intermediates *in Situ*



**Scheme 3.**  
Reactivity of Alkyl Amines